n-RiM: A Paradigm Shift in the Realization of Fully Inkjet-printed Broadband Tunable FSS using Origami Structures

Syed Abdullah Nauroze, Aline Eid, Manos M. Tentzeris
School of Electrical and Computer Engineering
Georgia Institute of Technology
Atlanta, Georgia 30332–0250
E-mail: nauroze@gatech.edu

***Abstract*—A state-of-the-art methodology for the realization of fully inkjet-printed tunable frequency selective surfaces using ripple-Miura (an origami) structure is presented. The dipoles are inkjet-printed along multiple foldlines of the ripple-Miura structure which facilitates systematic reduction in inter-element distance and an unprecedented transformation of the dipole elements into a ripple-shaped structure with folding. This results in substantial reduction in electrical length of the dipoles to realize wide range of resonant frequency and bandwidth tunability. The design also features an excellent angle of incidence rejection.**

***Index Terms*—Frequency selective surface (FSS), origami, Miura, tunable filters, inkjet-printing, cellulose paper, oblique incidence .**

I. Introduction

A Frequency Selective Surface (FSS) typically consists of a 2D or 3D periodic array of resonant elements on a substrate that filter certain bands of electromagnetic waves. The electromagnetic behavior of FSSs can be approximated by using equivalent circuit model theory which draws parallel between the actual FSS structure and its equivalent lumped component (LC) circuit. This simple yet accurate first-order circuit theory approach gives us good physcial insight into the working principle of FSSs and a good understanding of their band-stop or band-pass properties as a function of frequency and angle of incidence. The resonant frequency, bandwidth and bandpass/bandstop behavior of FSS is primarily determined by the size, shape and choice of the resonant elements as well as their inter-element distance whereas the effect of the dielectric can be ignored if its thickness is less than $\lambda/10$ [1].

Tradiationally tunable FSS structures realization usually involve either changing the electrical properties of the substrate [2] [3] or by placing varactors between the resonant elements [4]. These approaches are expensive, laborious and prone to failure in harsh environments. An alternative approach to realize on-demand tunable FSS has been presented in [5], which uses inkjet-printed dipoles across a single foldline of the origami structure that transforms into a V-shaped structure with reduced electrical length to achieve shift in resonant frequency. Even though this approach features wider frequency tunability range and higher angle of incidence rejection as compared to traditional approaches, it has limited bandwidth and a non-planar configuration that limits its usage in many practical applications. Moreover, the V-shaped structure has limited capability to add additional capacitance to each dipole to achieve resonant frequency shift.

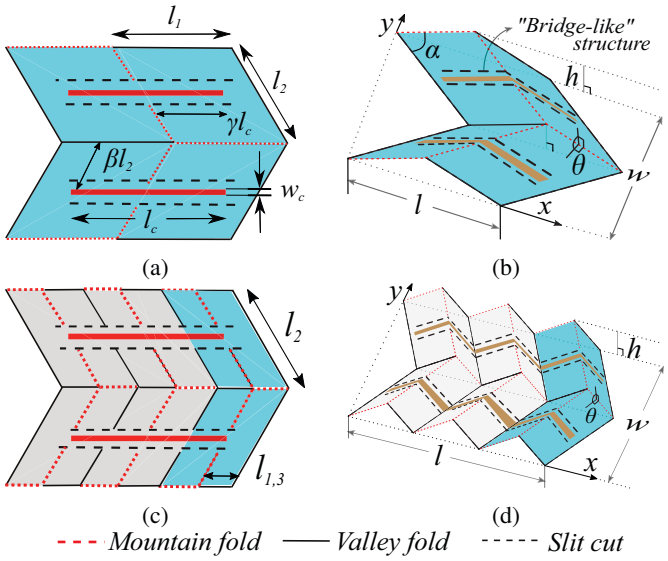

Fig. 1: Unit cell of 1-RiM in (a) flat state ($\theta = 180^o$) (b) folded state. Unit cell of 3-RiM FSS in (c) flat (d) folded state. $l_1 = 30mm$, $l_{1,3} = 10mm$, $l_2 = 20mm$, $\alpha = 45^o$, $\beta = \gamma = 0.5$, $l_c = 50mm$ and $w_c = 3mm$. Blue sections represents unit cell of a conventional Miura structure. $l_{1,n}$ denotes the length l_1 of each parallelogram of n-RiM unit cell

This paper presents a state-of-the-art methodology to realize fully inkjet-printed 4D tunable dipole-based FSS structures that use origami inspired structures to transform otherwise flat dipoles into ripple-shaped structures by placing them along multiple foldlines of the origami. Since the dipoles in this configuration span multiple foldlines they morph into a ripple-shaped structure (in a spatial meander-line fashion), it gives the proposed design a unique feature to add relatively more capacitance to the dipoles as compared to V-shaped dipoles [5]. As the ripple-shaped dipoles features significant reduction in electrical length, it facilitates substantial increase in the frequency tunability range and bandwidth of the overall structure. Special “bridge-like” structures are placed along the dipoles to improve their overall flexibility and ensure high conductivity without breakage for rugged usage and harsher environments. Three different ripple-Miura designs are simulated and measured to evaluate their performance with respect to different values of angle of incidence and folding configurations.

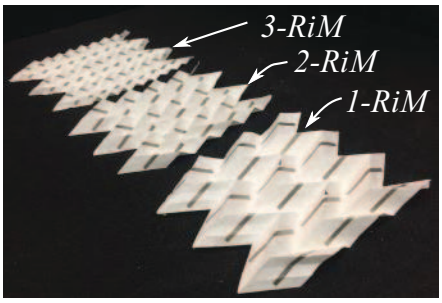

(a)

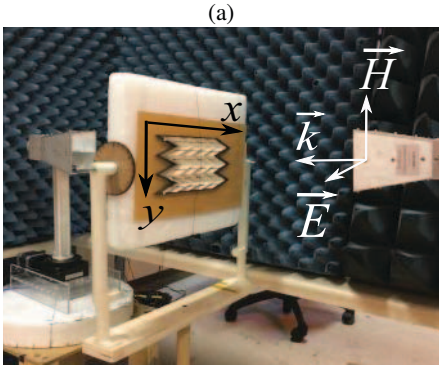

(b)

Fig. 2: (a) Three fabricated n-RiM FSS structures with n=1,2,3 (b) measurement setup

II. n-Ripple Miura (n-RiM) FSS with dipole elements

An origami-inspired inkjet-printed on-demand tunable dipole-based foldable FSS structure transforms 2D resonating elements of conventional FSS into a FSS with electrically small 3D resonating elements by using folding technique such as the Miura-Ori fold. The resultant FSS features an on-the-fly tunable frequency response with simple variation in its folding angle (θ). A typical Miura unit cell consists of four parallelograms (each with length l_1, l_2 and an internal angle α) that are connected to each other along their edges. The dipole elements are inkjet-printed across the Miura foldlines as shown in Fig. 1a to facilitate a systematic variation in their electrical length and inter-element distances with θ [5] [7]. A conventional Miura-FSS in Fig. 1b exhibits 15% frequency tunability as (θ) varies from 180^o (flat FSS) to 60^o (folded configuration)[5]. The shift in resonant frequency is mainly attributed to the change in the shape of dipole from a flat 2D structure to a 3D V-shaped structure which features smaller electrical length.

A further reduction in electrical length can be achieved by inkjet-printing each dipole (with the same initial length) on (n) multiple Miura unit cells with smaller dimensions - an n-**Ri**pple **M**iura (n-RiM). In this configuration, the dipole would span multiple Miura cells and hence it would morph into a ripple-shaped (meander-like) dipole as the RiM is folded. This results in dramatically increasing the frequency tunability range of the FSS structure by introducing extra capacitance at each fold of the dipole, a feature which is impossible to achieve using conventional FSS without adding non-linear components. Fig. 1c shows an example of a 3-RiM unit cell which consists of three conventional Miura unit cells with one of the dimensions of the parallelogram is three times smaller as compared to the original Miura unit cell (i.e $l_{1,3} = l_1/3 = 10mm$). Note that all other design parameters of the 3-RiM unit cell are similar to the original Miura unit cell, thus the two unit cells have equal overall areas. Another key advantage of using n-RiM is that it features an n times reduced overall height h, thereby making it more planar compared to the original Miura-FSS structure with relatively better frequency and bandwidth tunability.

The 3-RiM was fabricated by first perforating ripple Miura pattern outline on a $110\mu m$ thick cellulose paper; then, the dipoles were inkjet-printed across the foldlines using 10 layers of silver nanoparticle (SNP) ink and sintered at 150^oC for 2hrs to increase conductivity. Since cellulose paper absorbs SNP ink, the dipoles maintain a high conductivity at higher folding angles as they feature only minimal conductive trace breakage or cracking upon bending [6]. The flexibility of the dipoles is further enhanced by incorporating special "bridge-like" structures along the dipoles that allow dipoles to fold in a smoothened curved fashion along the foldlines rather than a sharp edge [5][7]. Finally, the ripple Miura pattern with dipoles is cut out and folded manually. It is important to note that in this paper a 3-RiM shown in Fig. 1d is considered for a 50mm long dipole as the highest RiM configuration since manually folding a n-RiM with $l_{1,n}$ less than 10mm becomes difficult. However, this process can be automated by using a temperature sensitive drafting paper [8].

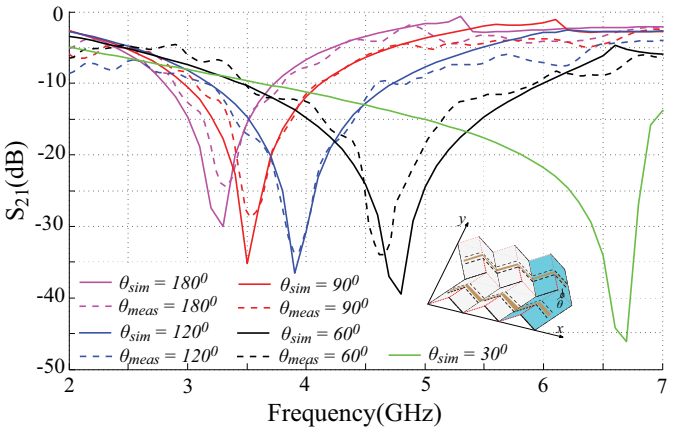

Fig. 3: Frequency response of a single-layer 3-RiM FSS structure ($l_{1,3} = 10mm$) for different values of folding angle (θ)

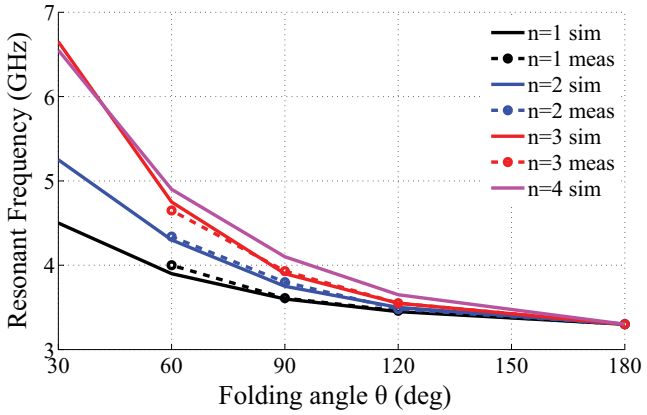

(a)

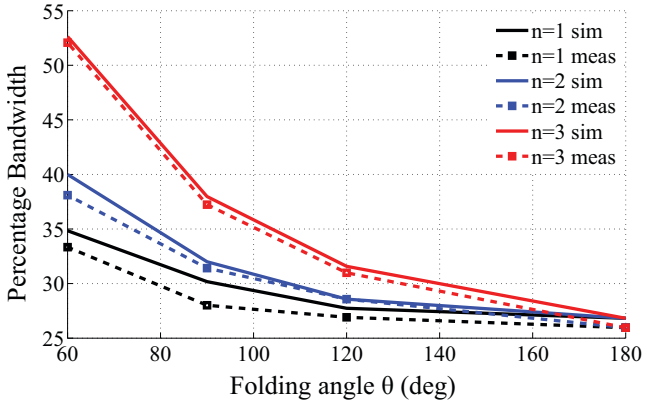

(b)

Fig. 4: Simulated and measured (a) resonance frequency and (b) percentage bandwidth of three n-RiM FSS structures (n=1,2,3) for different values of folding angle (θ)

III. Simulation and Measurement Results

The unit cells of three RiM structures (n=1,2,3) were designed and simulated in HFSS using master/slave boundary conditions with Flouquet ports. The simulated results were then verified using two broadband horn antennas in line-of-sight to each other while the RiM FSS structure is placed in the middle as shown in Fig. 2b. Specialized 3D-printed frames were used to hold the RiM FSS structure at different folding angles (θ=60^o, 90^o, 120^o) and ensure each unit cell has the same value of folding angle (θ).

The simulated and measured insertion loss (S_{21}) of 3-RiM FSS with respect to different values of the θ is shown in Fig. 3 which clearly indicates a systematic shift in the FSS frequency response as well as an increase in overall bandwidth due to folding. The resonant frequency shift is primarily caused by the reduction in the effective electrical length of the dipole elements while the bandwidth improvement is caused by the reduction in inter-element distance perpendicular to the axis of the dipole. Thus for a very high compression ($\theta = 30^o$) the frequency and bandwidth is increased exponentially which can be observed in Fig. 4a. It is important to note that this paper lists only simulated result for $\theta = 30^o$ to show that the same RiM structure can facilitate higher resonant frequency and bandwidth tunability when the structure is further compressed. The measurement of n-RiM structure at such high compression would require an extremely large RiM-FSS structures to avoid edge effects which becomes difficult to achieve with standard lab-size inkjet printer.

Similarly, the change in resonant frequency and percentage bandwidth for different n-RiM FSS structures for different values of folding angle (θ) is shown in Fig. 4 which indicates a distinctive increase in the range of the resonant frequency as well as of percentage bandwidth as θ is decreased (more compressed structure). Moreover, increasing the number of ripples (i.e. higher n values) further improves the tunability range and overall bandwidth of the FSS structure due to the introduction of additional capacitance caused by folding the RiM structure. However, in this case the maximum tunability limit is achieved for n=3 while adding more ripples to the Miura structure does not add a significant capacitance to shift the frequency at higher values, which can be observed in the Fig. 4a for $n = 4$ case.

It is worth noting over here that a single layer 3-RiM FSS structure features almost a 100% and 67 % increase in percentage bandwidth as compared to conventional dipole FSS and simple Miura-FSS ($n = 1$) structures, respectively. Similar bandwidths can only be achieved by realizing multiple layer configurations which require additional spacers, thereby increasing the overall volume of the FSS structure. On the other hand n-RiM has n times less volume compared to the Miura-FSS structure and can feature an almost planar structure by increasing number of ripples making it an attractive alternative to multiple layer traditional tunable FSS structures. In addition to that, the tunable range of the resonant frequency is increased by 44% compared to Miura-FSS which gives the designer an additional degree of freedom to design wideband highly tunable spatial filters.

The performance of 3-RiM with $\theta = 60^o$ for different values of angle of incidence (AoI) is shown in Fig. 5 which clearly

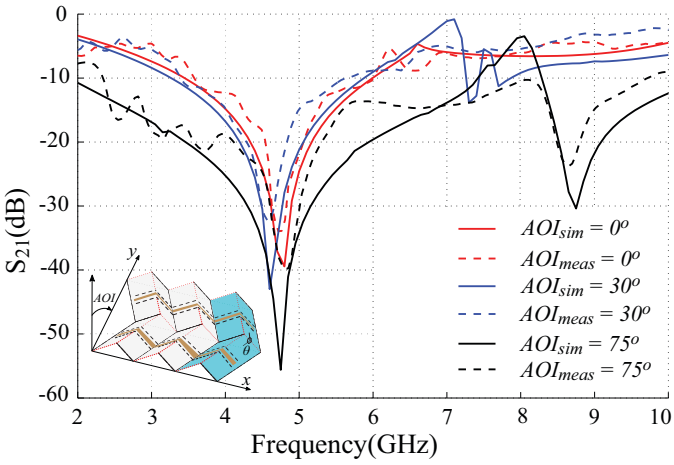

Fig. 5: Frequency response of a single-layer folded ($\theta = 60^o$) 3-RiM FSS for different values of angle of incidence

demonstrates a high AoI rejection for the proposed structure. Moreover, the overall bandwidth of the FSS structure increases to almost 116% at AOI=75^o which is twice as much as the normal incidence case. This is mainly because, at lower values of θ (i.e. when n-RiM is compressed), the dipoles have a 3D ripple-like structure which offers significantly higher mutual coupling (hence active impedance) between each ripple-dipole at larger scan angles (AoI values) as compared to the flat dipoles, thereby substantially improving the overall AoI rejection performance and bandwidth of the RiM-FSS. The appearance of a second harmonic at 9 GHz indicates excitation of odd-mode in the 3-RiM FSS structure [1] which is typically observed in dipole-based FSS structures at oblique angle of incidence.

IV. Conclusion

The paper presents a novel n-RiM FSS strcutures that feature a much superior bandwidth and frequency tunability performance as compared to traditional dipole FSS and previously reported origami-based FSS thereby presenting a complete paradigm shift in the realization of tunable FSS structures. It also demonstrates for the first time origami structures as a powerful tool to realize highly flexible, wideband and highly tunable structures without using any lumped components. The single layer 3-RiM FSS structure presented in this paper offers almost 100% increase in tunable range of resonant frequency while achieving a 200% increase in bandwidth as compared to traditional FSS structures - a feature that would typically require highly complex multilayer configurations. Moreover, unlike traditional 3D or origami-based FSS structures, an n-RiM FSS can be made extremely planar by introducing more ripples i.e. increasing n. A detailed analysis of n-RiM FSS structures with respect to change in folding angle (θ), number of ripples (n) and angle of incidence rejection is presented in this paper. The simulation and measurement results show a very good agreement with the theoretical values. The proposed design also demonstrates a substantial advantage of additive manufacturing technologies such as inkjet-printing since a similar structure would be almost impossible to realize using traditional manufacturing technologies. Moreover, its planar configuration would allow use in different applications such as smart skin, absorbers and design of radomes.

References

[1] B. A. Munk, "Frequency selective surfaces theory and design. john wiley&sons," 2000.

[2] T. K. Chang, R. J. Langley, and E. A. Parker, "Frequency selective surfaces on biased ferrite substrates," *Electronics Letters*, vol. 30, no. 15, pp. 1193–1194, Jul 1994.

[3] C. Mias, "Varactor-tunable frequency selective surface with resistive-lumped-element biasing grids," *IEEE Microwave and Wireless Components Letters*, vol. 15, no. 9, pp. 570–572, 2005.

[4] J. A. Bossard, D. H. Werner, T. S. Mayer, and R. P. Drupp, "A novel design methodology for reconfigurable frequency selective surfaces using genetic algorithms," *IEEE Transactions on Antennas and Propagation*, vol. 53, no. 4, pp. 1390–1400, April 2005.

[5] S. A. Nauroze, L. Novelino, M. M. Tentzeris, and G. H. Paulino, "Inkjet-printed "4d" tunable spatial filters using on-demand foldable surfaces," in *2017 IEEE MTT-S International Microwave Symposium (IMS)*, June 2017, pp. 1575–1578.

[6] S. A. Nauroze, J. Hester, W. Su, and M. M. Tentzeris, "Inkjet-printed substrate integrated waveguides (siw) with "drill-less" vias on paper substrates," in *Microwave Symposium (IMS), 2016 IEEE MTT-S International*. IEEE, 2016, pp. 1–4.

[7] S. A. Nauroze, J. G. Hester, B. K. Tehrani, W. Su, J. Bito, R. Bahr, J. Kimionis, and M. M. Tentzeris, "Additively manufactured rf components and modules: Toward empowering the birth of cost-efficient dense and ubiquitous iot implementations," *Proceedings of the IEEE*, vol. 105, no. 4, pp. 702–722, April 2017.

[8] G. J. Hayes, Y. Liu, J. Genzer, G. Lazzi, and M. D. Dickey, "Self-folding origami microstrip antennas," *IEEE Transactions on Antennas and Propagation*, vol. 62, no. 10, pp. 5416–5419, Oct 2014.